Prediction of Machining Induced Microhardness using Finite Element Simulations and Machine Learning in Titanium Alloys

Conference Paper · June 2013

CITATIONS
0

READS
168

3 authors:

Tuğrul Özel
Rutgers, The State University of New Jersey
185 PUBLICATIONS **9,654** CITATIONS
SEE PROFILE

Yigit M. Arisoy
Amazon
18 PUBLICATIONS **682** CITATIONS
SEE PROFILE

Durul Ulutan
California State University, Northridge
42 PUBLICATIONS **2,089** CITATIONS
SEE PROFILE

Prediction of Machining Induced Microhardness using Finite Element Simulations and Machine Learning in Titanium Alloys

Y.M. Arisoy, D. Ulutan and T. Özel*
Rutgers University, Department of Industrial and Systems Engineering, Piscataway, New Jersey 08854 USA
*ozel@rutgers.edu

Abstract

Titanium and its alloys are today used in many industries including aerospace, automotive and medical device. Ti-6Al-4V alloy is the most suitable because it offers favorable mechanical characteristics such as high strength-to-weight ratio, toughness, superb corrosion resistance and bio-compatibility. Titanium alloys are difficult-to-machine materials with considerable manufacturing problems such as machining induced surface integrity. In this study, the feasibility of predicting machining induced microhardness profiles by using finite element simulations and temperature-based machine learning predictive modeling has been investigated. 3D turning experiments are utilized to validate the FE simulation predictions. Predicted microhardness profiles are then utilized in understanding the effect of machining parameters such as cutting speed, tool material, coating and edge radius on the surface integrity. The study provides essential understanding in predicting machining induced microstructure alterations that are detrimental to fatigue life of titanium alloyed end products.

1. INTRODUCTION

Titanium alloys, specifically Ti-6Al-4V, are commonly used in the aerospace industry due to their high strength to weight ratio, toughness and corrosion resistance. They are also considered bio-compatible and can be used in medical devices. Surface integrity is one of the most relevant parameters used for evaluating the quality of finish machined surfaces, as the critical structural components in industry are manufactured with the objective to reach high reliability levels. Microhardness is an important aspect of surface integrity, and it can play an important role throughout the product's lifecycle as reviewed in [1].

Microhardness is affected by the machining induced strain, stress and temperature fields in the workpiece and although there are some analytical modeling efforts, they require a great understanding of the microstructure of the specific material and are not easily implemented [1,2]. However, it is known that machining parameters such as cutting speed, depth of cut, tool radius and tool coating have an effect on stress and temperature fields; therefore it is possible to obtain a relationship between the machining parameters and microhardness.

In a recent paper, Moussaoui et al. [3] investigated the effects of milling to microhardness and microstructure in Ti-6Al-4V. They state that machining causes a softening effect on the material due to high temperatures during cutting which cause Vanadium to diffuse into the α phase from the β phase of the alloy, without changing the microstructure. They also state that it is difficult to take traditional hardness measurements from two phase alloys such as the Ti-6Al-4V, and the results are dispersed. Jovanovic et al. [4] investigated how the mechanical properties and microstructure of investment cast Ti-6Al-4V change with different annealing temperatures and cooling rates. They found out that higher annealing temperatures and faster cooling rates yield higher tensile strength and hardness.

In this paper, as continuation of the study by Özel and Ulutan [5] on machining induced surface integrity where residual stresses were analyzed using experiments and 3D FE simulations, we perform microhardness analysis using similar experiments, simulations, and machine leaning based pseudo models in order to achieve an understanding about how cutting conditions affect the machining induced microhardness on Ti-6Al-4V titanium alloy.

2. EXPERIMENTAL WORK

2.1 Machining experiments

Face turning experiments, using four different cutting conditions and tools, were conducted on the Ti-6Al-4V specimen obtained as a cylindrical billet. To accomplish this, the specimen was machined in circular tracks, each track representing a different cutting condition with the same cutting tool. The machined face was then cut from the billet to form about 3 mm thick disk. The billet was then annealed at 704 °C and the surface was cleaned with a few finishing passes prior to starting a new set of experiments. This procedure was repeated using different tools (uncoated WC/Co and TiAlN coated WC/Co) until all disks were obtained with different tracks representing different cutting conditions and cutting tools. In the experiments, WC/Co inserts with edge radii of r_β = 25 µm, and TiAlN coated WC/Co inserts with edge radius of r_β = 10 µm have been tested in face turning of Ti-6Al-4V disks. A depth of cut of a_p = 2mm, two cutting speeds of v_c=55m/min and 90m/min, and two feeds of f = 0.05mm/rev and 0.1mm/rev were selected as cutting conditions.

2.2 Hardness measurements

Hardness measurements were taken on machined tracks of the disks using a Rockwell type tester in the HR15N scale and the values were then converted to Vickers Hardness (HV) scale. In some sets, some spreading was observed in hardness measurements. The measurements together with mean and standard deviation values are given in Table 1.

The workpiece was annealed at 704 °C in the furnace in between experiments, after each disk was cut off. Hardness measurements were taken from the untouched back surface of the cylindrical billet after each annealing process, and the mean and standard deviation are reported as 335.7 HV and 13.5 HV respectively. Hardness measurements were also taken from the workpiece after air cooling down to room temperature from 700 °C, 600 °C, 500 °C, and 400 °C. About thirty hardness measurements were taken for each case. The mean and standard deviation of hardness values for all cooled cases are shown in Figure 1 and Table 2.

Hot hardness measurements were performed on a cylindrical workpiece that was left over from the disk machining experiments. This piece also shares a surface that was used in taking the hardness measurements after annealing, allowing a valid comparison.

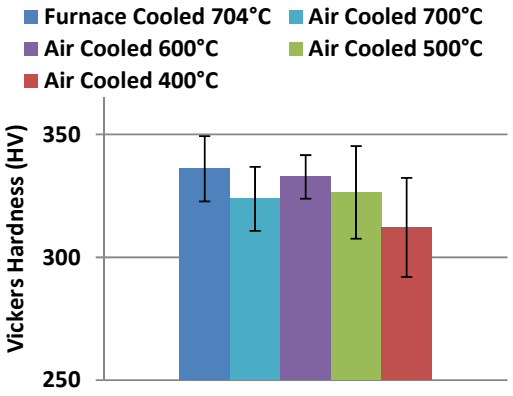

Figure 1: Hardness measurements at room temperature after cooling down.

Temperature measurements were taken with an infrared thermometer, and the values were fit into exponential curves to smooth the noisy data. Figure 2 shows the hardness versus temperature curves for each initial temperature. Hot hardness values were used to generate a temperature based instantaneous hardness model for the Ti-6Al-4V alloy, which is explained in Section 4. Note that the first measurements are not at the furnace heated temperature levels due to setup delays and machine measurement limitations.

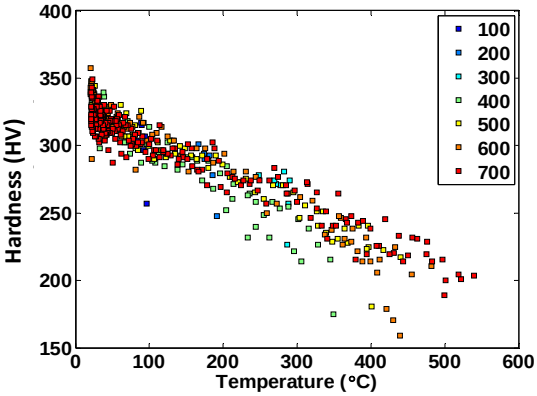

Figure 2: Hot hardness measurements for different initial temperatures.

3. FINITE ELEMENT ANALYSIS

3.1 Flow Stress Model

A constitutive model relating the flow stress to strain, strain rate and temperature is required for the simulations for the Ti-6Al-4V. This model is often obtained from the Split-Hopkinson pressure bar tests performed under various strain rates and temperatures, and is generally valid in certain ranges. The model given in Eq. (1) accounts for strain and strain rate hardening, temperature-dependent flow

softening and thermal softening effects and it is used in this work.

$$\sigma = \left[A + B\varepsilon^{n}\left(\frac{1}{exp(\varepsilon^{a})}\right)\right]\left[1 + Cln\frac{\dot{\varepsilon}}{\dot{\varepsilon}_0}\right]\left[1 - \left(\frac{T - T_r}{T_m - T_r}\right)^{m}\right]$$
$$\left[D_2 + (1 - D_2)\left[\tanh\left(\frac{1}{(\varepsilon + p_2)^{r}}\right)\right]^{s}\right] \quad (1)$$

where $D_2 = 1 - \left(\frac{T}{T_m}\right)^{d}$, and $p_2 = \left(\frac{T}{T_m}\right)^{b}$.

Here, σ is flow stress, ε and ε̇ are true strain and true strain rate, ε_o is reference true strain, and T, T_m and T_o are work, material melting and ambient temperatures respectively. The material model parameters are; A=725, B=300, n=0.65, C=0.035, m=1, a=0.5, b=2, d=0.5, r=12, s=-0.05. The melting temperature for Ti-6Al-4V is T_m = 1604°C.

3.2 FE Simulation Model

3D Finite Element software DEFORM is used with workpiece considered as viscoplastic and tool considered as rigid bodies. The workpiece has a 4-degree disk sector geometry with the same diameter used in the experiments and is discretized with 1.5x10^5 elements, giving a minimum element size of 0.005 mm as shown in Fig. 3. The tool is modeled using a small segment around the corner radius area of the cutting insert (r_ε=0.8 mm with 11° relief angle) and its mesh consists of 1.0x10^5 elements with minimum element size of 0.015 mm. The cutting zone and the tip of the tool have a very fine mesh in order to accurately represent the tool characteristics. Boundary conditions are defined for heat transfer from the workpiece to the tool. A very high heat conduction coefficient (h=100 kW/m^2/°C) is adopted to allow a rapid temperature change in the tool. Temperature-dependent material properties i.e. elasticity modulus E(T) (MPa), thermal expansion α(T) (1/°C), thermal conduction λ(T) (W/m/°C) and heat capacity C_p(T) (N/mm^2/°C) are used in simulations as shown in Table 3.

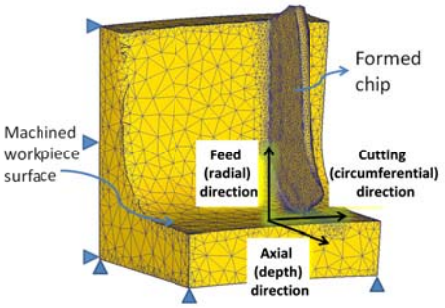

Figure 3: 3D FE model for machining.

The tool-chip contact friction is computed by a hybrid model where a shear region (with m=τ/k where τ is the shear stress and k is the shear flow stress) is defined around the tool edge radius curvature and a sliding region with the coefficient μ is defined along the rest of the rake face. The coefficients are taken as m=0.9 and $0.6 \leq \mu \leq 0.8$.

	Ti-6Al-4V	WC/Co	(Ti,Al)N
$E(T)$	0.7412T+113375	5.6x10^5	6.0x10^5
$\alpha(T)$	3.10^{-9}T+7.10^{-6}	4.7x10^{-6}	9.4x10^{-6}
$\lambda(T)$	7.039e$^{0.00117}$	55	0.0081T+11.95
$c_p(T)$	2.24e$^{0.00077}$	0.0005T+2.07	0.0003T+0.57

Table 3: Mechanical and thermo-physical properties of work and tool materials used in FE simulations [5].

The simulation output temperature fields have been obtained as shown in Figure 4 and are utilized in predictive modeling of microhardness profiles.

4. PREDICTIVE MODELING USING MACHINE LEARNING

4.1 Machine Learning

We consider using a machine learning based predictive model in order to find a relationship between the temperature of the workpiece during machining and the microhardness. In order to capture nonlinearities, machine learning algorithms can be used. Once properly configured, the machine learning algorithms inspect, extract and use the relationships and patterns that exist within the given dataset, which is very convenient for the user. Among machine learning algorithms, Random Forests (RF) method by proposed Breiman [6] is an adaptive nearest neighbor algorithm that can be used for classification and regression and it can easily capture nonlinear relationships between an input data set and a target data set. Regression trees work by recursively partitioning the data. Starting from the root node that contains the whole dataset, a tree is grown by generating two branches. The partitioning is done to minimize the sum of the squared errors over all splitting variables α (input parameters and predictor types) and split points β as shown in Eq. (2) where 1 and 2 denote the first and second regions respectively.

$$\min_{\alpha,\beta}\left[\sum_{i=1}^{N_L}(y_{i1} - \bar{y}_1)^2 + \sum_{i=1}^{N_R}(y_{i2} - \bar{y}_2)^2\right] \quad (2)$$

The splitting process continues at each new node until certain criteria are met; such as meeting a minimum error improvement δ for a split, or setting a minimum number of data points in each branch. When a node cannot be split anymore, it is called a terminal node or a leaf node. Usually, trees are grown until a minimum number of leaves exist. However,

overfitting is very common especially if the trees are fully grown. In this case, the bias will be small but small changes in the training data will yield a high variance due to the number of degrees of freedom in the tree. This can be prevented by pruning the trees but it will reduce the model's ability to capture complicated relationships in the data.

4.2 Prediction Methodology

The input and target vectors must first be determined carefully in order to train a model that achieves desirable results. Two separate RF models were constructed to predict instantaneous hardness during machining and final hardness of the workpiece after cooling down to room temperature. The training of the instantaneous model is performed using hot hardness measurements as the target vector, where the temperature and hardness values were measured and recorded. The input vectors are chosen as maximum temperature, instantaneous temperature and the cooling time. An input matrix is constructed by assigning each vector to a column such that each row is a different measurement. An RF regression model is trained using 800 trees. A representative tree from the model is shown in Figure 5.

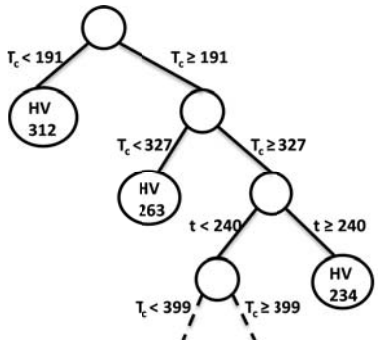

Figure 5: Representation of a regression tree in the instantaneous hardness model.

After the model is trained, FE simulation results are used as inputs to the model to obtain instantaneous hardness values during the machining operations. During the training of the model, 10% of the input data was reserved as test data and was not used in training. Figure 6 shows the goodness of the fit. The fit has R^2= 0.965, MAE=0.51 and RMSE=0.933. The secondary RF model is trained to calculate the hardness of the cooled down workpiece. A simple regression method could also be used for this phase.

For the prediction phase, FE simulation data are extracted in the form of nodal temperatures and passed to MATLAB. A line of 0.1 mm depth from the surface is selected close to the middle of the workpiece in order to see the effects of the tool. The workpiece and the line are shown in Figure 7.

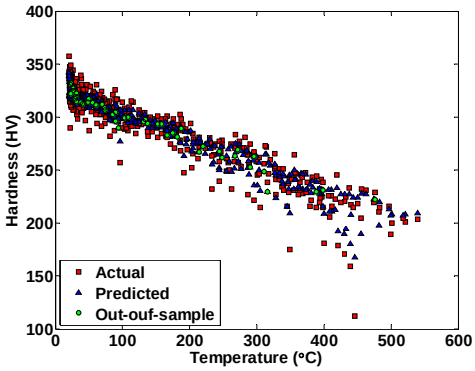

Figure 6: RF model fit for hot hardness.

The temperature data is interpolated using the available Delaunay triangulation in MATLAB without the use of element shape functions. The resulting data is fed into the RF model, and hardness values are calculated.

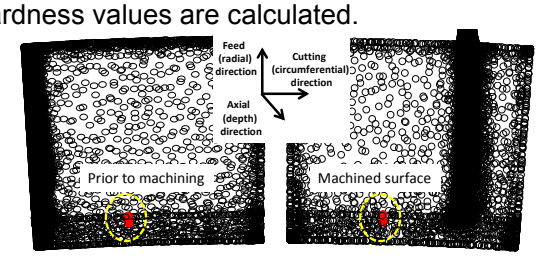

Figure 7: Representation in MATLAB.

It is important to note that current model is purely temperature dependent and is not intended to capture the work deformation induced effects. For instance, localized heating, an important factor that affects surface integrity during machining, is not present in the hot hardness measurements. Moreover, plastic deformation is not included in the current model. However, a more complicated and accurate model can be developed in a similar manner.

5. RESULTS

Simulations that are conducted at all eight cutting conditions are used in the hardness predictions. Two distinct steps of hardness predictions have been done. At first an instantaneous change in microhardness is computed based on the temperature rise. The evolution of temperature and hardness on the depth into the material line over time is shown in Figures 8 and 9 for a representative cutting condition (TiAlN coated tool, v_c= 90 m/min, and f=0.1 mm/rev condition).

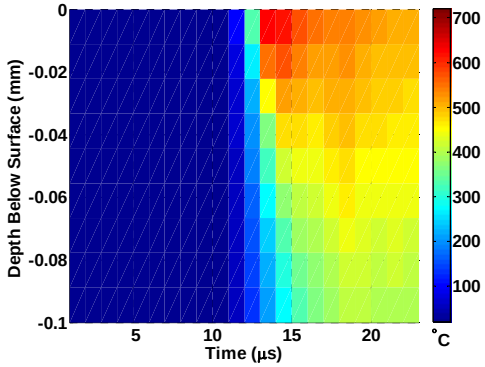

Figure 8: Temperature over line section on the workpiece during machining over time.

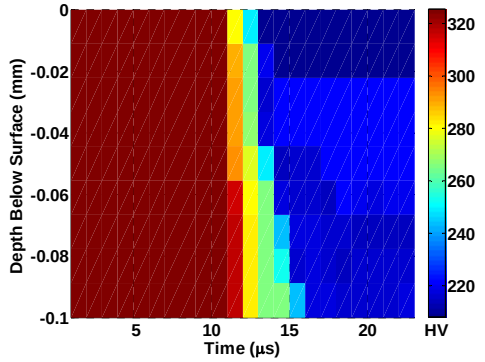

Figure 9: Hardness over line section on the workpiece during machining over time.

It is observed that the machined surface layer experiences an instantaneous hardness state due to localized heating during cutting process, and cools down to a lower temperature. During this repeated heating and cooling process, machined surface and subsurface go through changes in the microhardness. Microhardness state into the depth below the surface is shown just prior to chip formation (cutting) process for all cutting conditions in Fig. 9. Higher feeds create larger change in surface hardness while this effect diminishes after 50 µm depth into the machined surface. In general coated tool influences hardness more than uncoated tool.

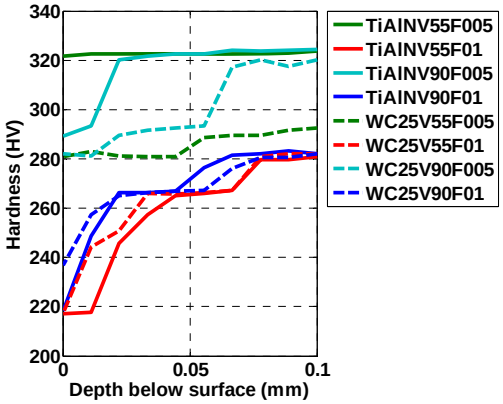

Figure 10: Instantaneous change in hardness prior to chip formation (cutting) process.

In addition, instantenous hardness change prior to and after the cutting process is also investigated. Machined surface is cooled down to the room temperature and resultant hardness profile is calculated as shown in Fig. 11. Higher feed rate and a larger edge radius are found responsible for greater alterations in microhardness profiles.

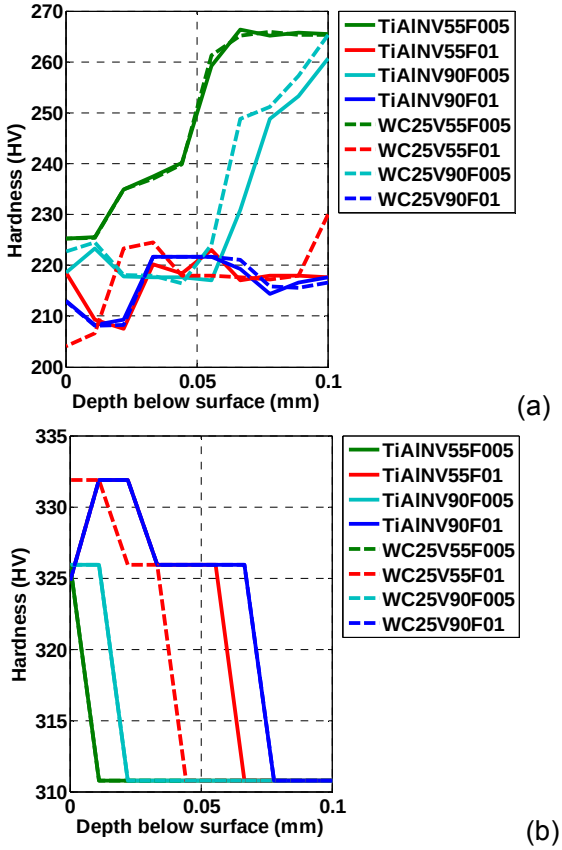

Figure 11: (a) Instantaneous hardness just after the cutting process and (b) hardness after cooling down to room temperature.

6. CONCLUSIONS

In this paper, machining induced hardness is investigated by using experiments, Finite Element simulations, and machine learning based predictive modeling in Ti-Al6-4V. It was found that the microhardness of the machined surface and subsurface is affected by the machining process and cutting conditions. A softening most likely due to grain coarsening occurs on the machined surface possibly due to high localized temperatures on the surface. The modeling approach proposed here will be extended to include deformation induced hardness alterations in the future studies.

7. ACKNOWLEDGEMENTS

This work is supported by NSF/CMMI-1130780.

8. REFERENCES

[1] Ulutan D, Özel T, 2011, Machining Induced Surface Integrity in Titanium and Nickel Alloys: A Review. International Journal of Machine Tools and Manufacture, 51: 250-280.

[2] Che-Haron CH, Jawaid A, 2005, The Effect of Machining on Surface Integrity of Titanium. Journal of Materials Processing Technology, 166:188-192.

[3] Moussaoui K, Mousseigne M, Senatore J, Chieragatti R, Monies F, 2012, Influence of milling on surface integrity of Ti6Al4V—study of the metallurgical characteristics: microstructureand microhardness, Int J Adv Manuf Technol, DOI 10.1007/s00170-012-4582-5.

[4] Jovanovic MT, Tadic S, Zec S, Miskovic Z, Bobic I, 2006, The effect of annealing temperatures and cooling rates on microstructure and mechanical properties of investment cast Ti–6Al–4V alloy, Materials and Design, 27: 192–199.

[5] Özel T, Ulutan D, 2012, Prediction of Machining Induced Residual Stresses in Turning of Titanium and Nickel Based Alloys with Experiments and Finite Element Simulations, CIRP Annals- Manufacturing Technology, 61/1: 547–550.

[6] Breiman L, 2001, Random Forests, Machine Learning, 45: 5–32.

Tool Type	Edge radius r_β (mm)	Feed f (mm/rev)	Cutting Speed v_c (m/min)	Mean Hardness (HV)	SD Hardness (HV)
WC/Co	25	0.05	55	301.57	16.02
WC/Co	25	0.1	55	316.85	8.87
WC/Co	25	0.05	90	316.68	18.91
WC/Co	25	0.1	90	310.01	37.90
TiAlN	10	0.05	55	326.49	9.50
TiAlN	10	0.1	55	323.29	17.39
TiAlN	10	0.05	90	319.05	13.28
TiAlN	10	0.1	90	324.20	16.27

Table 1: Hardness measurements on the machined tracks.

Condition	Temperature (°C)	Mean Hardness (HV)	SD Hardnesss (HV)
Furnace Cooled	704	335.75	13.27
Air Cooled	700	323.8	13.07
Air Cooled	600	332.78	8.87
Air Cooled	500	326.40	18.86
Air Cooled	400	312.14	20.10

Table 2: Hardness measurements at room temperature after cooling down

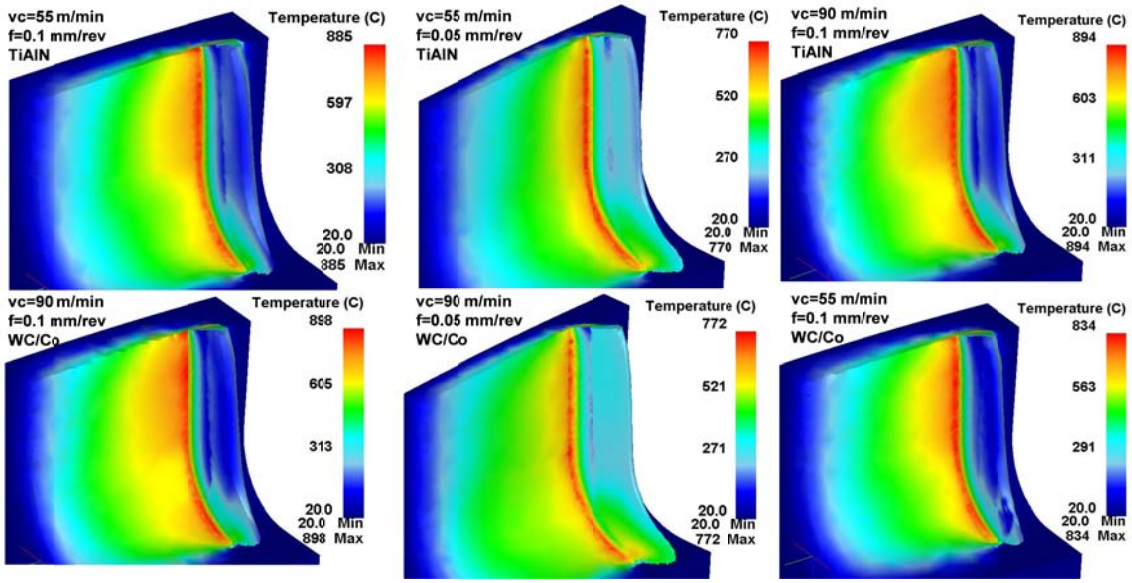

Figure 4: Predicted machining induced temperature fields using FE simulations.